Chemical Geology
September 2019, Volume 523 Pages 9-18
https://doi.org/10.1016/j.chemgeo.2019.05.033
https://archimer.ifremer.fr/doc/00859/97099/

Direct and indirect impact of the bacterial strain *Pseudomonas aeruginosa* on the dissolution of synthetic Fe(III)- and Fe(II)-bearing basaltic glasses

Perez Anne [1, *], Rossano Stéphanie [1, *], Trcera Nicolas [2], Verney-Carron Aurélie [3], Rommevaux Céline [4], Fourdrin Chloé [1], Agnello Ana Carolina [1, 5], Huguenot David [1], Guyot François [6]

[1] Université Paris-Est, Laboratoire Géomatériaux et Environnement, (EA 4508), UPEM, 77454 Marne-la-Vallée, France
[2] Lucia Beamline, Synchrotron SOLEIL, 91192 Gif-sur-Yvette, France
[3] Laboratoire Interuniversitaire des Systèmes Atmosphériques, UMR CNRS 7583/UPEC/UPD, IPSL, 94010 Créteil, France
[4] Aix Marseille Univ., Université de Toulon, CNRS, IRD, MIO UM 110, 13288 Marseille, France
[5] Centro de Investigación y Desarrollo en Fermentaciones Industriales, Calle 50 N°227, B1900AJL La Plata, Argentina
[6] Institut de Minéralogie, de Physique des Matériaux et de Cosmochimie, Muséum National d'Histoire Naturelle, CNRS, Sorbonne Université, IRD, 75005 Paris, France

* Corresponding author : Anne Perez, email address : anne.perez@u-pem.fr ; Stéphanie Rossano, email address : stephanie.rossano@u-pem.fr

Abstract :

This study investigates the direct and indirect bacterial contributions that influence the dissolution of basaltic glass. In this regard, three different types of glasses – with or without Fe, in the reduced Fe(II) or oxidized Fe(III) states – were prepared on the basis of a simplified basaltic glass composition. In order to prevent the direct contact between the glasses and the model siderophore-producing strain Pseudomonas aeruginosa, the glass samples were isolated in dialysis bags and immersed at 25 °C and pH 6.5 in bacterial cultures. Throughout the dissolution experiments, the following parameters were monitored: determination of bacterial growth, quantification of siderophore (i.e. pyoverdine) production, microscopic observation of the glass surface and determination of dissolution kinetics.

Isolating the glass from the bacterial suspension only triggered the biosynthesis of siderophores in the Fe(III)-bearing glass dissolution experiments. Siderophores were produced in the presence of Fe(II)-bearing and Fe-free glass, independently on the experimental setup. The siderophore production appeared to be either continuous in the absence of Fe (glass-free control, Fe-free glass dissolution experiments) or stopped as soon as the bacteria entered their stationary phase when an Fe source was present (Fe(II) and Fe(III)-bearing glass dissolution experiments). The increase in the dissolution rates of each glass was correlated to the complex stability constants of the siderophore with the metallic cations in presence ($K_{Fe2+} < K_{Al3+} \ll K_{Fe3+}$). Among the three glasses, only the Fe(III)-bearing one seemed to be significantly impacted by the dialysis process: its dissolution rate was doubled by isolating the glass grains from the cells. These results particularly allow to separate the impact of such bacterial exudates from physical contact effects: they showed the efficiency of pyoverdine in increasing the dissolution of an

Fe(III)-bearing glass and evidenced that a direct bacterial cell attachment to the surface of such a glass results in a more moderate enhancement of its dissolution process. This work is a new contribution regarding the high affinity of microorganisms for basaltic glasses as an Fe-source. It highlights the role of Fe(III) accessibility upon the bacterial cells as a key parameter regulating their activity and their efficiency in accelerating the dissolution.

Keywords : Basaltic glass, Pseudomonas aeruginosa, siderophore, bioalteration, dissolution kinetics

Introduction

Silicate glasses are abundant at the Earth's surface and notably near the oceanic ridge axes where large amounts of lava are emitted every year, generating a profusion of both amorphous and crystalline basaltic rocks. The alteration processes of basaltic glasses in permanent contact with seawater are known for partially controlling the composition of this latter but also the composition of the oceanic crust and impacting on the geochemistry of the Earth mantle. The alteration of basaltic glasses could also have a significant impact on the Earth's climate by contributing to the sequestration of atmospheric CO_2 through carbonation processes resulting from the dissolution of the glass and the release of earth alkali elements (Berner et al., 1983). Understanding the alteration mechanisms of the oceanic crust at low temperatures is thus essential to implement the Earth surface mass-balance studies and then improve the geochemical models predicting the evolution of our planet (Hart, 1970; Staudigel and Hart, 1983; Spivack and Staudigel, 1994; Gislason and Oelkers, 2003).

During the last two decades, the high diversity and the abundance of the microorganisms living at the subsurface of oceanic basalts were evidenced (Thorseth et al., 2001; Santelli et al., 2009; Mason et al., 2009; Orcutt et al., 2011; Henri et al., 2015; Sudek et al., 2017). As basaltic glasses represent one of the most profuse sources of Fe and also contain additional elements (Mg, Ca, K…) required for microbial nutrition (Staudigel and Hart, 1983), they are suspected to sustain the development of microbial communities (Sudek et al., 2009). These elements representing a nutritive potential can be: 1/ adsorbed or 2/ incorporated inside the bacterial cells, 3/ trapped within the biofilms or 4/ complexed with bacterial exometabolites such as siderophores (e.g. Uroz et al., 2009). However, the role of basaltic glasses as a substantial source of nutrients, the impact of such microbial activity on their dissolution rates and its potential control on the biogeochemical cycling of elements at the rock/water interface is still a matter of debate (Templeton et al., 2005; Cockell et al., 2010; Henri et al., 2016).

Numerous laboratory studies were dedicated to the understanding of the basaltic glass dissolution processes in a broad range of abiotic experimental conditions (e.g. Guy and Schott, 1989; Daux et al., 1997; Techer et al., 2000, 2001; Oelkers, 2001; Oelkers and Gislason, 2001; Stroncik and Schmincke, 2001; Gordon and Brady, 2002; Crovisier et al., 2003; Gislason and Oelkers, 2003; Wolff-Boenisch et al., 2004a; Flaathen et al., 2010; Verney-Carron et al., 2011; Parruzot et al., 2015; Perez et al., 2015, Ducasse et al., 2018). The dissolution of basaltic glass is traditionally described by two simultaneous mechanisms, whose predominance notably depends on the pH of the aqueous fluid: (1) an ion exchange between network-modifying elements of the glass (Na, K, Ca, Mg) and hydrogenated species from the solution (interdiffusion) and (2) the hydrolysis of the bonds linking oxygen atoms to network-forming elements of the glass (Si, Al, Fe(III)). Dissolution can also be presented as the breaking of all metal-oxygen bonds (from the weakest to the strongest) until the structure is completely destroyed (Oelkers, 2001; Oelkers and Gislason, 2001). The rate-limiting step of the basaltic glass dissolution process is the detachment of tetrahedral Si near the glass surface. However, the preferential release of other network-forming elements (Al, Fe) is assumed to influence the

destabilization of the glass network. For these reasons, the impact of the introduction in the liquid medium of biomolecules known for their high affinity with such cations should be investigated.

Several field studies conducted in deep-sea water and dedicated to the characterization of microbial communities showed that many cultured organisms display at least two of the tested functions: heterotrophy, Fe(II) and Mn(II) oxidation and siderophore production (e.g. Sudek et al., 2009). This demonstrated that such microorganisms are metabolically and functionally versatile, which supports their adaptability to extreme environments. Siderophores are molecules produced when bacteria are submitted to a nutrient stress, and especially to a high need in Fe. The biosynthesis of siderophores involves several steps catalysed by specific enzymes in different locations from cytoplasm to periplasm, from where they are secreted to the extracellular medium (Schalk and Guillon, 2013). Siderophores have generally a very high affinity for two among the major network-forming elements Al and Fe(III). In previous studies (Perez et al., 2015, 2016), Fe-bearing basaltic glasses (MORB2, MORB3) and Fe-free glass (HAPLO) have been shown to exhibit enhanced dissolution rates in the presence of siderophores and then in the presence of the model siderophore-producing strain *Pseudomonas* (*P.)* compared to abiotic control experiments. The results highlighted the promoting role of organic ligands as complexing agents, and particularly of pyoverdines, which are the siderophores specifically produced by *P. aeruginosa*. These conclusions were in agreement with numerous abiotic studies dealing with dissolution kinetics of minerals/oxides/silicate glasses in the presence of organic molecules (Welch and Ullman, 1992; Watteau and Berthelin, 1994; Stillings et al., 1995; Drever and Stillings, 1997; Kraemer et al., 1999; Liermann et al., 2000; Cocozza et al., 2002; Cheah et al., 2003; Wolff-Boenisch, 2007; Wang et al., 2005; Olsen and Rimstidt, 2008; Martinez-Luevanos et al., 2011; Torres et al., 2014; Akafia et al., 2014; Lazo et al., 2017). This promoting effect is in favour of the occurrence of a bacteria-mediated process, which notably contrasts with several recent studies attesting to a small or negligible impact of the presence of bacteria on dissolution kinetics of minerals (Hopf et al., 2009; Hutchens, 2009; Sverdrup, 2009; Bray et al., 2015) and of basaltic glass (Wolff-Boenisch, 2011; Stockmann et al., 2012). This promoting effect was observed in specific conditions (growth phase and nutrient free systems) in which the acquisition of nutrient was crucial for the bacterial cells. Even though the impact of siderophores on the dissolution kinetics of basaltic model glasses was evidenced, the global bacteria-promoted dissolution mechanisms of the glasses remain hard to define as bacteria can also directly interact with glass surfaces or produce other metabolites that could influence the dissolution rates (Ullman et al., 1996; Hutchens, 2009; Shirokova et al., 2012; Ahmed and Holmström, 2015; Cornu et al., 2017; Wang et al., 2018).

The present work aims to specifically explore the indirect dissolution mechanisms of basaltic glass by bacteria. For this purpose, bioalteration experiments were performed on HAPLO, MORB2 and MORB3 synthetic glasses, in which dialysis bags were used to prevent a direct contact between the model siderophore-producing strain *P. aeruginosa* and the basaltic glasses tested. Throughout the dissolution experiments the bacterial growth and the production of siderophore (*i.e.* pyoverdine) were monitored and coupled with the microscopic observation of the glass surface and the calculation of dissolution kinetics.

Material and Methods

1. Samples

The theoretical compositions of the three model glasses used in this study are given in Table 1. The MORB2 and MORB3 glasses were prepared according to a simplified typical *Mid Oceanic Ridge Basalt* composition and contain mainly Fe(II) and Fe(III), respectively. The HAPLO glass is a Fe-free equivalent composition in which Fe is mainly substituted by Mg.

Table 1: Nominal compositions of the synthetic Fe(II)-bearing glass (MORB2), Fe(III)-bearing glass (MORB3) and Fe-free glass (HAPLO) of interest.

	MORB2 & 3 (wt %)	**HAPLO** (wt %)
SiO_2	48.6	51.6
Al_2O_3	15.7	16.7
FeO	12.5	0.0
CaO	11.1	11.8
MgO	7.7	15.2
Na_2O	2.7	2.9
TiO_2	1.4	1.5
K_2O	0.2	0.3

MORB2, MORB3 and HAPLO glasses were prepared (DRX, XAS, BET measurements) as described in the work of Perez et al. (2016). Fe(II) content was estimated to range between 10 and 30 at.% of total iron in MORB3 and around 90 at.% of total iron in MORB2.

2. Bioalteration experiments

P. aeruginosa ATCC® 9027 (Sigma Aldrich) bacteria were first grown 30 hours under agitation (160 rpm) and 25°C in 2 mL of Lysogeny Broth (LB) medium, a nutritionally rich medium containing: 10 g L^{-1} tryptone, 5 g L^{-1} yeast extract, 5 g L^{-1} NaCl. This freshly grown culture of *P. aeruginosa* was then used for the bioalteration experiments.

The bioalteration experiments have been carried out in a MM9 medium (pH 6.5) whose composition was adapted from Schwyn and Neilands (1987) and Liermann et al. (2000). Near neutral conditions of pH were chosen to allow for comparison with similar experiments conducted in abiotic conditions (Perez et al., 2015). The MM9 medium is composed of 6.06 g L^{-1} Na_2HPO_4, 0.3 g L^{-1} KH_2PO_4, 0.5 g L^{-1} NaCl, 1.0 g L^{-1} NH_4Cl and 50 mM Bis Tris. The initial pH was adjusted by adding HCl 1 M. The solutions were sterilised and cooled to 25 °C. They were then supplemented with 0.2% (v/v) 1 M $MgSO_4$ (final concentration 2 mM), 1% (v/v) filter-sterilised (cellulose filter, Ø0.2 µm) 20% (w/v)

glucose (final concentration 1 M) and 0.01% (v/v) 1 M $CaCl_2$ (final concentration 0.1 mM); these solutions were prepared and sterilized separately. No Fe was detected in the prepared growth medium and no precipitate formation was observed. Dissolution experiments were performed in sterile erlenmeyers closed with cotton plugs to allow free passage of air over the edge of the vessels and to maintain an aerobic aqueous environment. These experiments consisted in mixing a volume of 250 mL of MM9 medium was with 0.625 g of glass powder. All experiments were inoculated with 125 µL of the same LB culture of *P. aeruginosa* in order to start the bioalteration test with bacteria having identical age and initial nutritional status. The cultures were continuously agitated at 160 rpm. The glasses were isolated from the bacterial suspension by sterile dialysis bags (®CelluStep T4). Porous dialysis membranes allow small solutes to pass while large species are retained and can thus effectively be used as a separation process based on size rejection. The Molecular Weight Cut Off of the membranes used in our experiments is 12000-14000 Da, which means that: (1) 90% of the species whose molecular weight ranges between 12000 and 14000 Da do not pass the membrane and do not access to the glass surfaces and (2) 100% of the species whose molecular weight exceeds 14000 g/mol do not pass the membrane. In the context of this study, the used membranes allow most exometabolites, in particular siderophores (200 - 2000 Da), to interact with the glass surface whereas the bacteria cells are isolated from the solid samples.

For each glass, abiotic experiments (without introducing *P. aeruginosa*) were conducted following the same protocol but without dialysis bags. They are mentioned as “abiotic control” in the Results and Discussion sections. Moreover, *P. aeruginosa* was cultivated in identical conditions but without adding the glass into the system. These glass-free experiments were mentioned as “glass-free control” in the following sections.

All experiments (abiotic control, glass-free control and experiments with glass contained in dialysis bags) were performed in duplicates.

At selected dissolution times, 2.3 mL of the liquid medium were filtered (cellulose acetate filter, Ø0.2 µm) and kept for Inductively Coupled Plasma and Optical Emission Spectroscopy (ICP-OES) analysis whereas 1.7 mL were placed in a spectrophotometer cell for Optical Density (OD) measurements and 200 µL were plated right away on LB agar medium for the microbial counting procedure. Sampling times were chosen as a function of the bacteria growth: frequent from the beginning until the end of the exponential phase and then more distant (0.6, 1, 1.6, 2, 3 and 5.7 days). The pH was checked after 5.7 days of each experiment. pH variations were within 10% of the initial pH values and were considered as negligible. Experiments were extended until 15 days and 1.7 mL were sampled at days 8, 10, 13 and 15 to allow supplementary measurements.

3. Analysis

3.1. ICP-OES analysis

The amounts of dissolved Al, Fe and Si were analysed using a Perkin Elmer Optima 8300 ICP-OES. Measurements were performed using emission wavelength at 288.16 nm (Si), 308.22 nm (Al), 239.56 nm (Fe). Ca, Mg, Na, K were exempted from analysis being initially present in significant amounts in the growth medium.

For each element and at each dissolution time, the normalized mass loss NL_i from the glass into the solution was calculated using Eq. (1).

$$NL_i = \frac{[i]}{\left(\frac{S}{V}\right)\times x_i} \quad (1)$$

where *[i]* is the concentration (mg L^{-1}) of the element *i* in solution, *S* the initial surface of the glass powder in contact with the fluid, *V* the volume of solution and x_i the mass percentage of the element *i* in the glass.

Considering a linear regression, the initial slope of the curve was calculated in order to evaluate the *apparent* initial rate of dissolution r_i as given in Eq. (2):

$$r_i = \frac{dNL_i}{dt} \quad (2)$$

The speciation code CHESS (Van der Lee et al., 2003) was used to calculate the elemental speciation in solution. The combined thermodynamic database is that of CHESS (based on the EQ3/6 database).

3.2. Bacterial growth and siderophore detection

At each sampling time, total biomass growth was estimated by measuring the Optical Density (OD) of the incubated medium at 600 nm and by the Colony Forming Unit (CFU) count procedure. After 2.7 days (respectively 2.9 days for MORB3 glass) and 5.7 days, dilutions of the bacterial medium were plated on LB agar and incubated 24 h at 25 °C for the counting step while the sampled solution was also filtered (cellulose acetate filters, Ø0.2 µm) and placed into a spectrophotometric cell. Optical spectra were recorded between 300 and 600 nm. Identical spectrophotometric cells were used for all measurements, with a standard optical path length.

3.3. SEM observations

In order to visually investigate the potential direct effect of bacteria at the surface of our glasses, experiments without dialysis bags were performed without any sampling procedure. After 6 days, the glasses were dried following a critical point dying (CPD) protocol in order to avoid the damaging

effects of surface tension on bacterial cell and biofilm potentially present at the glass surface. 250 µL of glass in suspension in the bacterial medium were mixed with 4 mL of 0,05 M 4-(2-hydroxyethyl)-1-piperazineethanesulfonic acid (HEPES) solution (pH 8) and then slowly injected in a swinnex® containing a polycarbonate filter (Ø 0,22 µm). The glass grains and bacterial cells were retained on the filter and successively washed with 5 mL of 50%, 70%, 96% and 100% ethanol (vol.). The filter was carefully kept in an absolute ethanol bath then introduced in a CPD chamber *(Leica EM CPD300)* and submitted to 20 cycles (CO_2 injection, increase of temperature and pressure and depressurisation) of 4 min each. After being dried, the samples were immediately carbon coated and observed with Scanning Electron Microscopy (*Zeiss Ultra55* microscope) with a filament tension of 2 kV.

Results

1. *Bacterial growth and siderophore production*

1.1. *Growth and Fe release*

Optical densities (ODs) at 600 nm of the sampled solutions and CFU counting are plotted versus time in Figure 1 for the three glasses. The absorbance of a bacterial medium at 600 nm (OD) is correlated to the number of suspended cells within the liquid medium as it characterizes the turbidity of the solution. OD values are in good agreement with the CFU counting. Correlation factors between OD and CFU values have been calculated for each experimental condition and are equal to 0.97 (Control), 0.94 (MORB3), 0.99 (MORB2) and 0.94 (HAPLO).

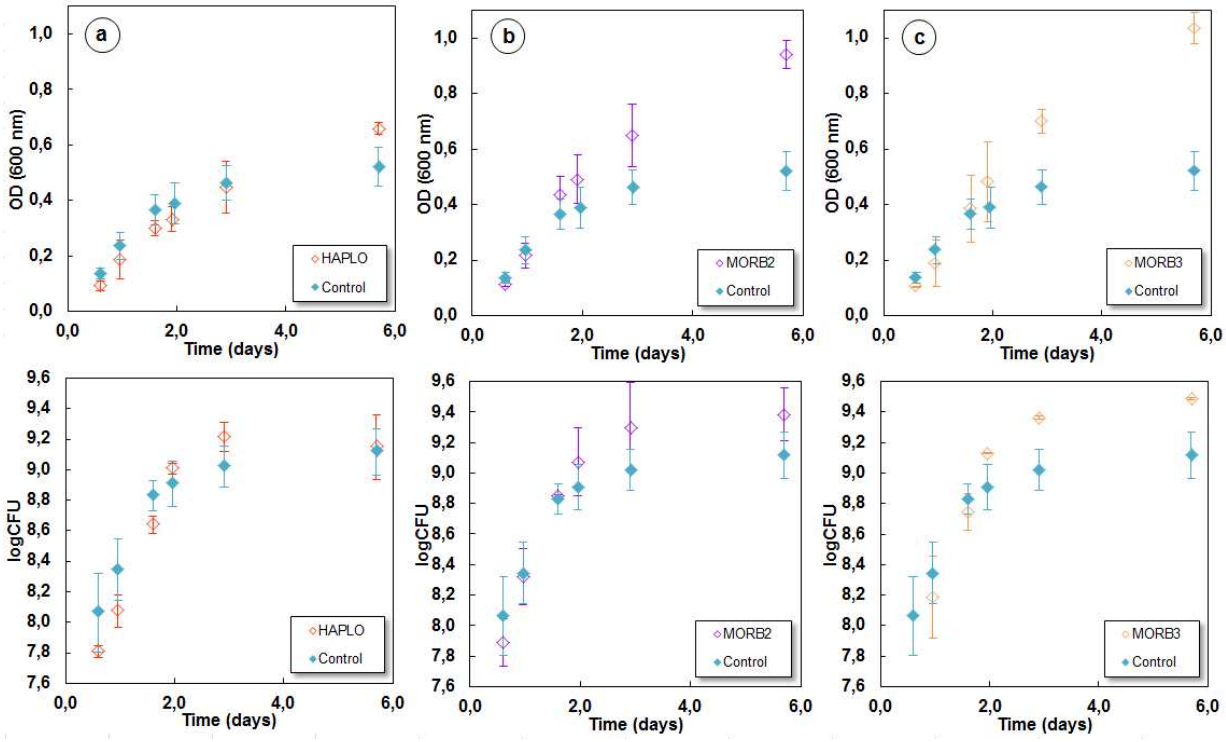

Figure 1: Bacterial growth curves (measured optical densities at 600 nm or Colony Forming Units versus time) of *P. aeruginosa* culture in the presence of the HAPLO (a), MORB2 (b) and MORB3 (c) glasses confined in dialysis bags. Full blue data points represent the glass-free control experiment. Growth experiments in MM9 were performed in duplicates and error bars correspond to ± standard deviation (SD) between the 2 measured values.

The experiments in the presence of the HAPLO glass exhibit growth curves very close to those obtained in the control experiments (Figure 1a). The bacterial growth is more pronounced compare to glass-free control when bacteria are incubated with Fe-bearing glasses (Figures 1b & 1c).

The averaged Fe concentrations measured in the cultures incubated in the presence of MORB2 and MORB3 glass isolated from the bacterial suspension by dialysis membranes are plotted versus time in Figure 2 and compared to the results of abiotic control experiments.

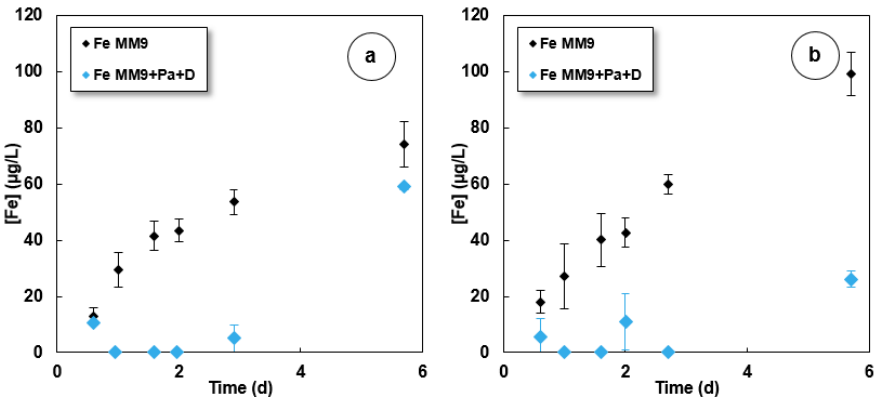

Figure 2: Fe concentrations in aliquots sampled during the dissolution of MORB2 (a) and MORB3 (b) glasses at 25°C in sterile control experiments (MM9) at pH 6.5 and in a bacterial culture of *P. aeruginosa* (Pa) isolated from the glass by dialysis bags (D). Each point represents the average between two duplicate values and error bars are equal to ±SD.

At the difference with dissolution experiments of the same glasses in ultrapure water (UPW) (Perez et al., 2015), Fe concentration levels in solution are most of the time above the ICP-OES detection limit. Basic speciation calculations (CHESS code) show that, regarding the abundant presence of phosphate salts in the MM9 medium, Fe is mainly present as soluble $FeHPO_4^{+}_{(aq)}$, as suggested by Pokrovsky et al. (2009a,b).

In abiotic conditions (Fe MM9), Fe is continuously released in the medium all along the experiment from both glasses. By contrast, in the presence of the strain (Fe MM9+Pa+D), Fe is almost non-detected from 0.6 to 5.7 days, which is correlated to a fast cell division step (Figure 1).

1.2. Siderophore production

Pyoverdines can be detected between 380 and 420 nm with a UV-Vis spectrophotometer through the observation of a two-shoulder characteristic absorption peak (Meyer and Abdallah, 1978). The absorbance spectra of all bacterial cultures, recorded in the 380 - 420 nm region are plotted in Figure 3.

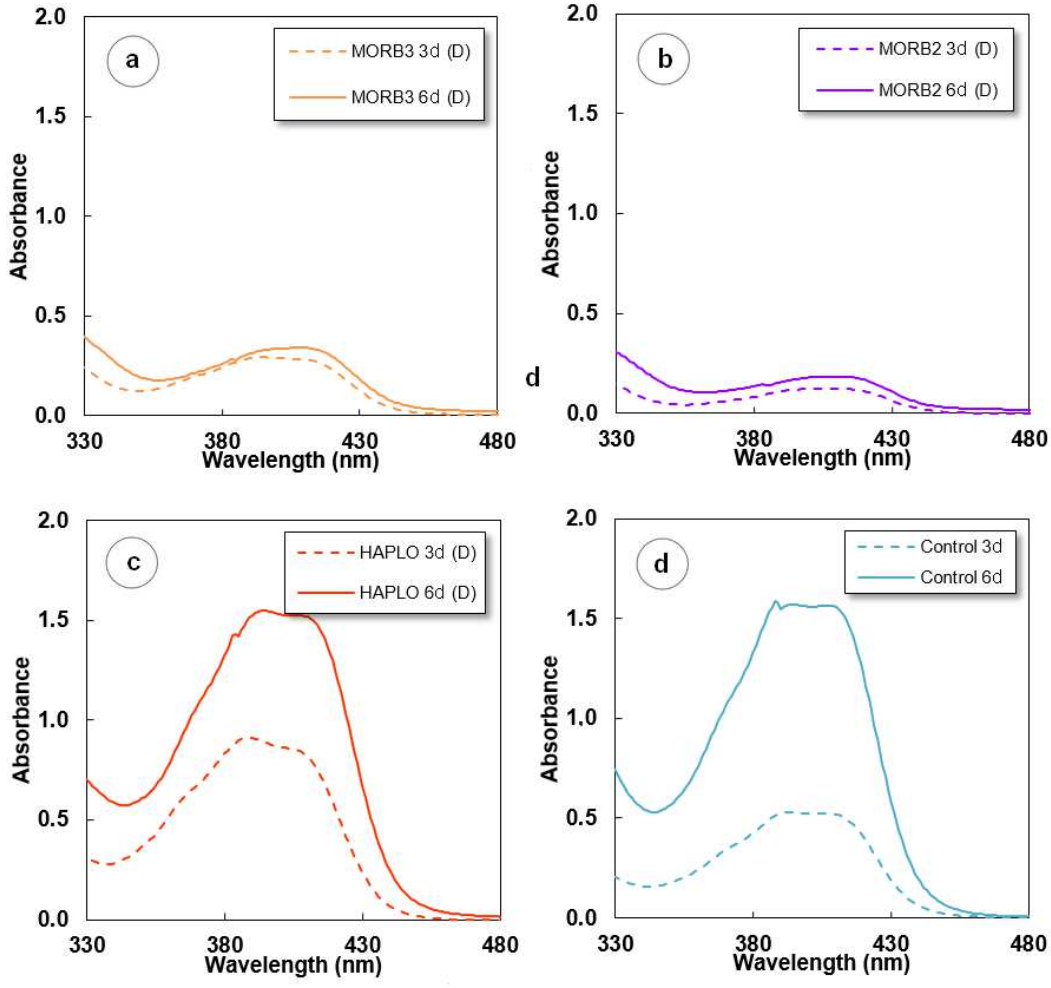

Figure 3: UV Absorption spectra of the MM9 6.5 bacterial medium in the absence (Control) (d) or the presence of the MORB3 (a), MORB2 (b), and HAPLO (c) glasses contained in dialysis bags, recorded at 3 days (3d) and 6 days (6d) of the experiments.

According to the shape of the recorded spectra, pyoverdine molecules are detected in all experiments.

On the basis of the measured absorbance value at 405 nm (A_{405}), an estimated free pyoverdine concentration can be calculated according to the Beer Lambert law:

$$[PVD] = \frac{A_{405}}{19000} \times 10^6 \qquad (3)$$

The pyoverdine is characterized by different molar extinction coefficients depending on its form in solution. The coefficient of free pyoverdine (19000 L/mol/cm) is lower than that of Fe^{3+}-pyoverdine complexes (26000 L/mol/cm) and greater than that of Al^{3+}-pyoverdine complexes (18000 L/mol/cm). As it is not possible to experimentally distinguish between the free pyoverdine, Fe^{3+}-pyoverdine and Al^{3+}-pyoverdine fractions, approximate values of total pyoverdine concentrations in solution were calculated by using the molar extinction coefficient of free pyoverdine given in Equation (3) and are given in the Table 2:

Table 2: Apparent pyoverdine concentrations $[PVD]_{ap}$ (in µM) in glass-free control experiments and in dissolution experiments of HAPLO, MORB2 and MORB3 glasses after 6 days of incubation. The reported values are averaged concentrations calculated from the two replicate series of experiments and the reported error is equal to ±SD.

	$[PVD]_{ap}$
Control	80.3 ± 2.6
HAPLO	77.4 ± 3.7
MORB2	13.9 ± 6.3
MORB3	19.7 ± 2.6

The highest amounts of pyoverdine in the incubated media mixed with glasses are detected in the HAPLO glass experiment, with pyoverdine concentrations after 6 days around 80 µM. The shape and the position of peak is the same after 3 and 6 days. These results are very close to those obtained in the glass-free control experiments (Figure 3d). Both control and HAPLO are Fe-free systems.

Regarding the MORB2 glass, the absorbance spectra presented in Figure 3b show closed intensity values (corresponding to pyoverdine concentration of ~15 µM according to Table 2) either at 3 and 6 days, by contrast to the experiments with the HAPLO glass, in which pyoverdine seems to be produced continuously from 0 to 6 days of incubation. The spectra recorded at days 3 and 6 mainly differ by a change in the shape of the absorption peak of pyoverdine species (Figure 3b). In order to highlight this evolution, absorbance spectra of the cultures recorded until 15 days of incubation for MORB2 experiments are represented in Figure 4.

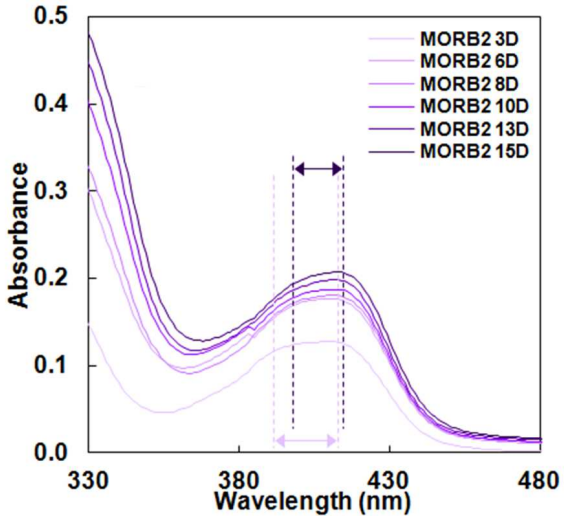

Figure 4: Absorption spectra of the MM9 6.5 bacterial medium in the presence of the MORB2 glass contained in dialysis bags, recorded at 3, 6, 8, 10, 13 and 15 days (D) of the experiments. The arrows materialize the shift of the pyoverdine absorption region toward higher wavelengths with time.

The spectra show a constantly-evolving signal with time (shifted toward higher wavelengths and changing into a one-shoulder peak). At near neutral pH condition, this one-shoulder shape characterizes the presence of Fe^{3+}-pyoverdine complexes (Albrecht-Gary et al., 1994). Such an evolution could attest for the continuous formation of Fe^{3+}-pyoverdine complexes in solution.

Finally, Figure 3a shows that bacterial cells isolated from the MORB3 glass grains produce pyoverdine over the course of the experiments. Pyoverdine concentration after 6 days of experiments in the incubated medium is estimated to be lower than or equal to 20 µM (Table 2). Figure 5 illustrates the change in the shape and the position of the absorption peak of pyoverdine throughout 15 days of experiments.

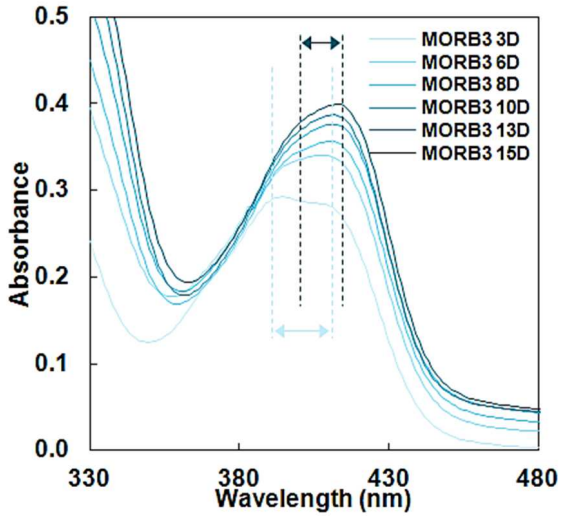

Figure 5: Absorption spectra of the MM9 6.5 bacterial medium in the presence of the MORB2 (a) and MORB3 (b) glasses contained in dialysis bags, recorded at 3, 6, 8, 10, 13 and 15 days (D) of the experiments. The arrows materialize the shift of the pyoverdine absorption region toward higher wavelengths with time.

As observed for the MORB2 glass experiment, the two-shoulder peak characteristic of free-pyoverdine continuously evolves towards the single absorption peak of Fe^{3+}-pyoverdine complexes. Similarly to the MORB2 glass experiments and by contrast with the HAPLO ones, in which pyoverdine concentrations within the liquid medium are almost doubled from day 3 to day 6, the siderophore production in the MORB3 systems seems to slow down between day 3 and day 15. This decrease in siderophores production rates correlates with the entering in the stationary phase of growth of *P. aeruginosa* (Figure 1).

2. Dissolution rates

The NLs of Si, Al and Fe in all experiments are plotted versus time in the Supplementary Data file. Considering that a fraction of Al and Fe, dissolved from the glasses, is likely to be scavenged by the bacterial cells and/or adsorbed at their surface (and in consequence not taken into account by ICP-OES measurements), the dissolution rates of the three glasses will be discussed on the basis on Si data.

Apparent dissolution rates calculated in abiotic control experiments and in *P. aeruginosa* (with glass confinement) based on Si concentrations measured in the liquid media are given in Table 3.

Table 3: Apparent dissolution rates (mg/m^2/d) based on Si release from the three glasses in abiotic control experiments and in biotic experiments with glass confinement. The reported values are average rates calculated from the two replicate series of experiments and the reported error is equal to ±SD.

	Abiotic control experiments	**Biotic experiments**
HAPLO	2.6 ± 0.1	4.9 ± 0.2
MORB2	2.4 ± 0.1	5.2 ± 0.3
MORB3	2.6 ± 0.1	7.3 ± 0.7

The presence of bacteria in the aqueous medium (MM9) has a positive impact on the global dissolution of the three glasses: the Si release rates are enhanced by a factor of 1.5 to 3 depending on the experimental conditions. The dissolution rates calculated from Si concentration in the three experimental systems are enhanced by comparison with abiotic systems in the order: HAPLO ≈ MORB2 < MORB3.

3. SEM observation

The SEM images of the surface of a MORB3 glass sample incubated 6 days in the presence of *P. aeruginosa* without dialysis bags (direct contact) are presented in Figure 6. They are compared to images of a MORB3 glass surface acquired after 6 days of dialysis-using experiments and to images of the surface of an HAPLO glass submitted to 6 days of dialysis-free experiments.

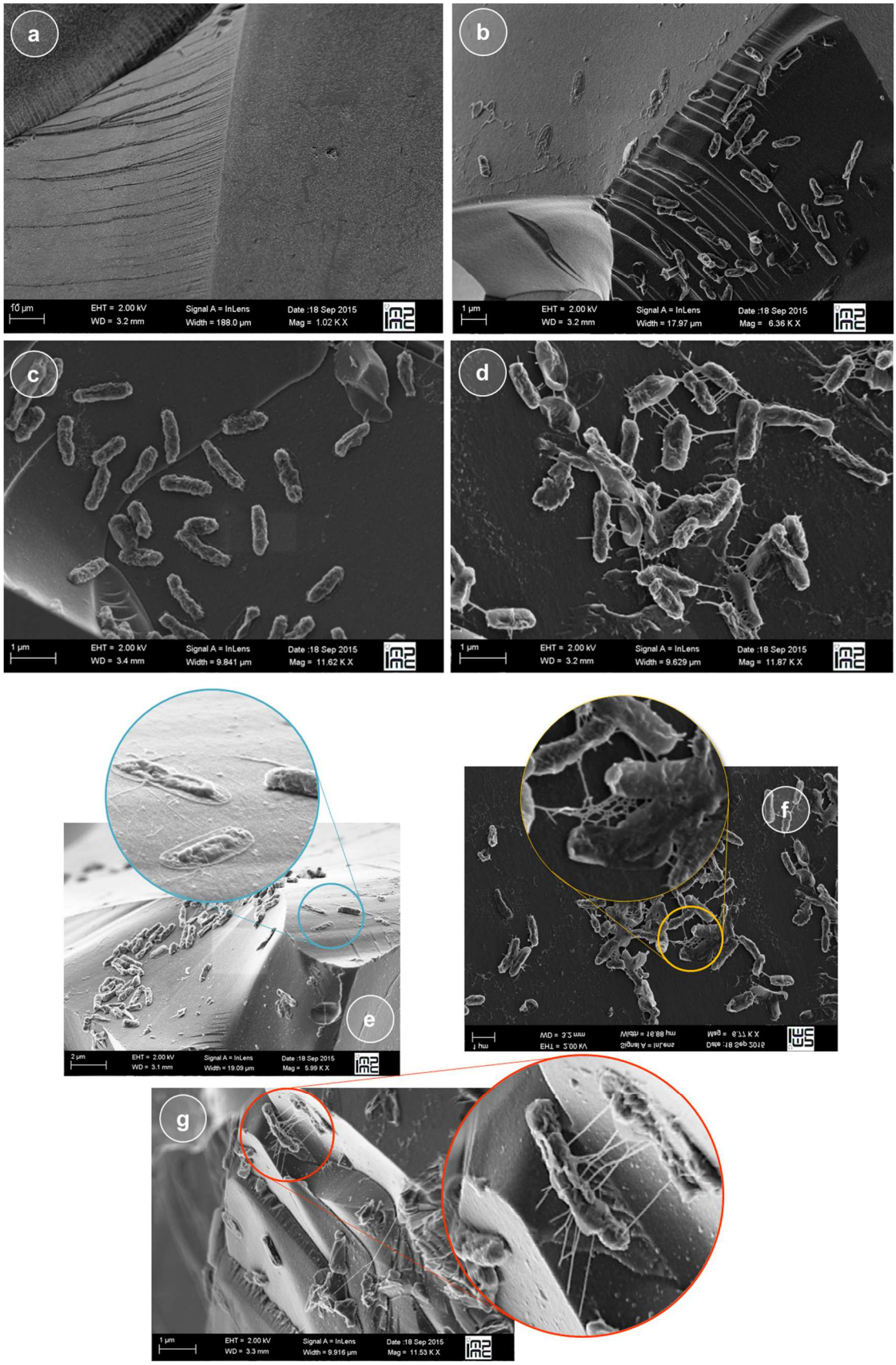

Figure 6: SEM images showing the comparison between 1/ the MORB3 glass surface after 6 days of dialysis membranes (a) and membranes-free (b) experiments and 2/ the HAPLO (c) and MORB3 (d, e, f, g) glass surface after 6 days of membranes-free experiments.

If bacteria do not seem to massively colonize the surface, they are however homogenously present on the grains of both types of glass, by contrast with dialysis bag experiments, in which no bacteria cells is observed. The comparison with the HAPLO glass (Figure 6c and 6d) highlights the development of biofilms only on Fe-bearing glass surfaces. The MORB3 images show that the cells are strongly attached to the glass, as dead cell residues remain at the surface after the CPD protocol (Figure 6e). They also show that biofilm communities start to develop: bacteria produce filamentous structures that allow them to progressively connect to each other (Figure 6f) and to the surface of the glass (Figure 6g).

Discussion

In this section, the results will be in several places compared to those presented by Perez et al. (2016), obtained by dissolving the three glasses without isolating them from the bacterial suspension. This comparison will only be used with the aim to highlight new aspects of basaltic glass dissolution in the presence of the model strain *P. aeruginosa.*

1. Indirect use of Fe-bearing glass by bacteria

The more pronounced growth of *P. aeruginosa* when bacteria are incubated with Fe-bearing glasses compare to Fe-free systems (control and HAPLO dissolution experiments) is correlated with the non-detection of Fe with the liquid medium during the bacteria exponential phase of growth. This strongly suggests the nutritive potential of Fe-bearing glasses for the strain. This result is notably in strong agreement with our previous study (Perez et al. 2016) and with a study by Sudek et al. (2017). In this latter, the authors evidenced the elevated growth of *Pseudomonas stutzeri VS 10* incubated in the presence of basaltic samples in comparison with basalt-free experiments. This suggests that an Fe-bearing glass could be a nutrient source for *P. aeruginos*a in exponential phase of growth, even if it is isolated from the bacterial suspension by the dialysis membranes.

2. Evidence of direct bacteria/glass interactions

Among the three glasses, only MORB3 seems to be significantly impacted by the dialysis separation. Its dissolution rate increases from 4.0 ± 0.2 mg/m^2/d (Perez et al., 2016) to 7.3 ± 0.8 mg/m^2/d by isolating the glass from the cells. Apparent pyoverdine concentrations in dialysis (D) and no dialysis-using experiments (Perez et al., 2016) are confronted in Figure 7.

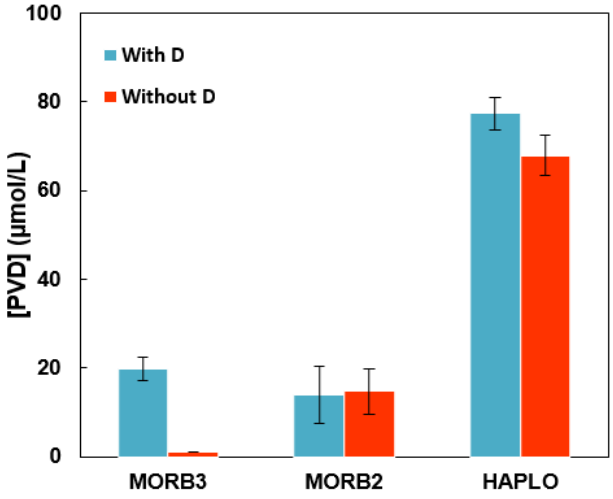

Figure 7: Apparent concentrations in pyoverdine in HAPLO, MORB2 and MORB3 systems after 6 days of experiments with/without dialysis (D) membranes (Perez et al., 2016). The reported values are averages concentrations calculated from the two replicate series of experiments and the reported error is equal to ±SD.

Pyoverdine is produced in similar amounts independently on the presence of dialysis bags in the MORB2 and HAPLO dissolution experiments, by contrast with the MORB3 dissolution experiments in which pyoverdine is only detected when the glass is confined in the bags. This result particularly shows the significant bacterial dependence on the glass composition and notably on the redox state of Fe within the glass.

The results of the experiments without dialysis bags (Perez et al., 2016) showed that without any separation between the MORB3 glass and the bacterial suspension, the Fe fraction abiotically released in solution was lower than the Fe fraction measured within the bacterial cells. This result suggests that, in the presence of the strain, the Fe fraction naturally released from the glass into the liquid medium is entirely assimilated by the bacteria and that even more Fe is mobilized from the glass through a non-identified biological process. The absence of siderophore in the system indicated that pyoverdine molecules were not responsible for enhancing the Fe release.

When the glass is separated from the bacterial suspension, a significant pyoverdine production by the cells is observed. This production of pyoverdine in presence of dialysis membranes is a good indicator of a high bacterial need in Fe, not observed when the bacteria can access to the glass. It could be then hypothesized that the biological process that enhances the Fe release from the MORB3 consists in direct glass surface/bacteria interactions. These specific interactions are materialized on the SEM images displayed in Figure 6. The comparison with the HAPLO glass surface after the same duration of incubation and the absence of biofilm in such experimental case highlights the affinity of bacterial cells with the MORB3 surface, on which bacteria start to settle *via* exopolymers networks. Very similar biofilm patterns were presented in the work on *Pseudomonas stutzeri* of Sudek et al. (2017) between 4 and 7 days of incubation with basaltic glass samples.

Studies focusing on discriminating the direct/indirect impact of bacteria are rare as most experimental works on bioweathering is carried out using mineral or glass grains in suspension within the liquid medium. Oulkadi et al. (2014) worked on the development on a silica gel with dialysis properties embedding various phyllosilicate particules and were able to separate the effect of cell attachment and the impact of several exudates. Ahmed and Holmström (2015) carried out bioalteration tests on biotite in microplate devices with porous insert preventing the access of several bacterial strains to the mineral. By contrast with the results described in the present study, siderophores were detected in all experimental conditions (with/without bacterial separation) and the authors systematically measured increased dissolution rates when bacteria could access to the glass. Dialysis membranes were also used in 2007 by Buss et al. to discriminate microfeatures on iron silicate surfaces corresponding to direct bacterial effect or to pitting caused by siderophore-promoted dissolution and in 2012 by Shirokova et al. regarding the dissolution of olivine. In our case, the used of dialysis membrane is also promising as it allows, in the MORB3 systems, the quantification of the impact of direct cell attachment.

3. Siderophore concentrations and dissolution rates

If it demonstrates the impact of bacterial cells attachment on the dissolution rates of Fe(III)-bearing glass, the addition of a dialysis system in the experiments presented in the work by Perez et al. (2016) also brings new highlights regarding the impact of siderophores in basaltic glass dissolution rates:

First of all, the presence of pyoverdine molecules has a significant catalyzing effect on the dissolution of the three types of glass. This effect is evidenced by the comparison between dialysis and no dialysis-using MORB3 experiments. Without dialysis membranes, the lowest bacterial impact on the dissolution kinetics among all the tested glasses (4.0 ± 0.2 mg/m^2/d from Perez et al. (2016)) is correlated with the non-detection of pyoverdine in the system (Figure 4). These experiments show that the moderate enhancement relative to the experiment without bacteria is caused by a direct bacteria/glass interaction. By contrast, the dialysis-membrane-using experiments, in which low but significant amounts of pyoverdine (around 20 µM) are detected in solution, are characterized by the highest Si release rate (7.3 ± 0.8 mg/m^2/d, Table 3). In the HAPLO and MORB2 dissolution experiments, in which pyoverdine is systematically detected, the Si release rates are also increased compared to sterile experiments. The non-effect of the presence of the dialysis membranes on the dissolution rates of these glasses suggests that the dissolution is indirectly enhanced by the production of organic molecules by the strain, likely pyoverdine molecules.

Secondly, the observed effect of pyoverdine correlates well with the complex stability constants of the siderophore with the metallic cations in presence ($K^{Fe^{2+}} < K^{Al^{3+}} \ll K^{Fe^{3+}}$) (Albrecht-Gary et al., 1994; Chen et al., 1994; Hernlem et al., 1996; Szabo et Karkas, 2011). In particular, the siderophore has the most significant effect on the dissolution rates when the cations that are the most likely to form complexes with it are involved as network-forming elements in the glass structure (Al^{3+}, Fe^{3+}). This

suggests that complexation reactions between pyoverdine and structural Al and/or Fe promote the dissolution either by a surface-controlled mechanism (Cocozza et al., 2003) or by increasing the solubility of these metallic elements in solution (Oelkers and Schott, 1998). Such siderophore-promoted dissolution is in good agreement with studies dedicated to the interactions between desferrioxamine-B and Fe(III)-bearing minerals/glasses (Reichard et al., 2005; Wolff-Boenisch and Traina, 2007; Cervini-Silva, 2008; Haack et al., 2008; Dehner et al., 2010; Perez et al., 2015, Torres et al., 2018). However, there is only a limited number of existing studies exploring the promotion of mineral/glass dissolution by other siderophores and notably pyoverdine (Ferret et al., 2014; Parello et al., 2016; Perez et al., 2016). This work particularly contributes to show the efficiency of pyoverdine in increasing the dissolution of an Fe(III)-bearing glass.

Finally, the correlation between the effect of pyoverdine on the dissolution kinetics and the complex stability constants does not seem to depend on the concentrations of pyoverdine in the systems. As an example, pyoverdine has the highest impact on dissolution rates of the MORB3 glass despite a progressively decreasing siderophore production process and a maximum concentration in the medium equal to 20 µM (Table 2, Figure 3, a recapitulative figure is also given in the Supplementary Data section). By contrast, it has a lower impact on the dissolution kinetics of the HAPLO glass although it is continuously produced by the cells and its concentration approximates 70-80 µM after 6 days of dissolution (Figure 3).

In a basaltic environment where Fe solubility is low and where siderophore-producing strains are commonly detected, the biosynthesis of these complexing agents might operate as a mechanism developed to ensure nutritional Fe-availability. Nevertheless, the extrapolation of these results to natural systems has to be considered with prudence. Even if they tend to demonstrate that low amounts of siderophores might be sufficient to experimentally observe a bacterial-mediated enhanced dissolution, such results may overestimate the real impact of microorganisms. Moreover, this *in vitro* impact, obtained in experiments where specific bacteria are grown in experimental conditions designed for siderophore production, is shown to increase by less than one order of magnitude the dissolution rate of the glass samples. The experimental investigation of the chemical weathering of basaltic glass in more representative liquid media and/or with an environmental bacterial consortium is needed to ensure the effectiveness of the glass-weathering potential evidenced in all its forms by this work.

Conclusion

This work attests of the impact of bacteria on the dissolution kinetics of three synthetic basaltic model glasses. Isolating the samples from the bacterial suspension was essential to unravel the mechanisms/kinetics by which bacteria impact on the dissolution of basaltic glass. The results showed that siderophores were produced in all experiments with dialysis, stopped as soon as the bacteria reached a stationary phase of growth for the Fe-bearing glasses and continuously increasing for the

Fe-free glass. A limited quantity of pyoverdine molecules in solution (around 20 µM) was sufficient to significantly improve the dissolution rate of the MORB3 glass, which was increased by three times as compared to abiotic control experiments. By contrast, the dissolution kinetics of Fe(II)-bearing and Fe-free glass incubated with *P. aeruginosa* were not impacted by the non-access of bacteria to the glass.

This work is a new contribution regarding the high affinity of microorganisms for basaltic glasses as an Fe-source. It brings new evidences of the positive impact on the dissolution kinetics of such a glass composition, on the importance of Fe redox state within the glass for bacterial-mediated processes. It also highlights the strategies developed by the bacteria to acquire Fe, depending on the form under which it is primarily available to them: 1/ as structural Fe within the glass network, directly accessible (no-dialysis experiments), 2/ as not accessible structural Fe (dialysis experiments), 3/ directly in solution, forming soluble complexes with phosphates initially present within the liquid medium (in both types of experiments, the “abiotically” released fraction of Fe was shown to be entirely assimilated by the growing bacteria). For each Fe source, siderophore production is shown to mediate the dissolution process.

Acknowledgements

This work was supported by grants from Region Ile de France and by CNRS-INSU (INTERVIE).

References

Akafia M.M., Harrington J.M., Bargar J.R. and Duckworth O.W. (2014) Metel oxyhydroxide dissolution as promoted by structurally diverse siderophores and oxalate. *Geochim. Cosmochim. Acta* **141**, 258-269.

Ahmed E. and Holmström S. J. M. (2015) Microbe-mineral interactions: The impact of surface attachment on mineral weathering and element selectivity by microorganisms. *Chem. Geol.* **403**, 13-23.

Albrecht-Gary A., Blanc S., Rachel N., Ocaktan A., Mohamed A. and Abdallah A. (1994) Bacterial iron transport: coordination properties of pyoverdine PaA, a peptidic siderophore of *Pseudomonas aeruginosa*. *Inorg. Chem.* **33**, 6391-6402.

Berner R.A., Lasaga A.C., Garrels R.M. (1983) The carbonate-silicate geochemical cycle and its effect on atmospheric carbon dioxide over the past 100 million years. *Am. J. Sci*. **283**, 641-683.

Bray A.W., Oelkers E.H., Bonneville S., Wolff-Boenisch D., Potts N.J., Fones G. and Benning L.G. (2015) The effect of pH, grain size, and organic ligands on biotite weathering rates. *Geochim. Cosmochim. Acta* **164**, 127-145.

Buss H.L., Lüttge A. and Brantley S.L. (2007) Etch pit formation on iron silicate surfaces during siderophore-promoted dissolution. *Chemical Geology* **240**, 236-342.

Callow B., Falcon-Suarez I., Ahmed S. and Matter J. (2018) Assessing the carbon sequestration potential of basalt using X-ray micro-CT and rock mechanics. *International Journal of Greenhouse Gas Control* **70**, 146-156.

Cheah S., Kraemer S., Cervini-Sila J. and Sposito G. (2003) Steady-state dissolution kinetics of goethite in the presence of desferrioxamine-B and oxalate ligands: implications for the microbial acquisition of iron. *Chem. Geol.* **198**, 63-75.

Cockell C. S. et al. (2010) Microbial endolithic colonization and the geochemical environment in young seafloor basalts. *Chem Geol* **279**, 17–30.

Cocozza C., Tsao C.C.G., Cheah S.F., Kraemer S.M., Raymond K.N., Miano T.M. and Sposito G. (2002) Temperature dependence of goethite dissolution promoted by trihydroxamate siderophores. *Geochim. Cosmochim. Acta* **66**, 431-438.

Cornu J.Y., Huguenot D., Jézéquel K., Lollier M. and Lebeau T. (2017) Bioremediation of copper-contaminated soils by bacteria. *World Journal of Microbiology and Biotechnology* **33**.

Crovisier J., Advocat T. and Dussossoy J.L. (2003) Nature and role of natural alteration gels formed on the surface of ancient volcanic glasses, natural analogs of waste containment glasses. *Journal of Nuclear Materials* **321**, 91-109.

Daux V., Guy C., Advocat T., Crovisier J. L. and Stille P. (1997) Kinetic aspects of basaltic glass dissolution at 90°C: role of aqueous silicon and aluminium. *Chem. Geol*. **142**, 109-26.

Dessert C., Dupré B., Gaillardet J., François L.M. and Allègre C.J. (2003) Basalt weathering laws and the impact of basalt weathering on the global carbon cycle. *Chem. Geol.* **202**, 257-273.

Drever J. and Stillings L. (1997) The role of organic acids in mineral weathering. *Colloids and Surfaces* **120**, 167-181.

598 Ducasse T., Gourgiotis A., Pringle E., Moynier F., Frugier P., Jollivet P. and Gin S. (2018) Alteration of
599 synthetic basaltic glass in silica saturated conditions :Analogy with nuclear glass. *Applied*
600 *Geochemistry* **97**, 19-31.

601 Ferret C. (2014) Siderophore-promoted dissolution of smectite by fluorescent Pseudomonas.
602 *Environmental Microbiology Reports* **6**, 459-647.

603 Flaathen T., Gislason S. and Oelkers E. (2010) The effect of aqueous sulphate on basaltic glass
604 dissolution rate. *Chem. Geol.* **8**, 345-354.

605 Gislason S. R. and Oelkers E. H. (2003) Mechanism, rates and consequences of basaltic glass
606 dissolution: II. An experimental study of the dissolution rates of basaltic glass as a function of pH and
607 temperature. *Geochim. Cosmochim. Acta* **67**, 3817-3832.

608 Gordon S.J. and Brady P.V. (2002) In situ determination of long-term basaltic glass dissolution in the
609 unsaturated zone. *Chem. Geol.* **190**, 113-122.

610 Guy C. and Schott J. (1989) Multisite surface reaction versus transport control during the
611 hydrolysis of a complex oxide. *Chem. Geol.* **78**, 181-204.
612
613 Hart R. (1970) Chemical exchange between sea water and deep ocean basalts. *Earth Planet Sci Lett*
614 **9**, 269–279.
615
616 Henri P., Rommevaux-Jestin C., Lesongeur F. and Ménez B. (2016) Structural iron (II) of basaltic
617 glass as an energy source for Zetaproteobacteria in an Abyssal Plain Environment, off the Mid Atlantic
618 Ridge. *Frontiers in Microbiology* **6**, 1518.

619 Hopf J., Langenhorst F., Pollok K., Merten D. and Kothe E. (2009) Influence of microorganisms on
620 biotite dissolution: an experimental approach. *Chemie der Erde – Geochemistry* **69**, 45-56.

621 Hutchens E. (2009) Microbial selectivity on mineral surfaces: possible implications for weathering
622 processes. *Fungal Biology Reviews* **23**, 115-121.
623 Kraemer S., Cheah S., Zapf R., Xu J., Raymond K. and Sposito G. (1999). Effect of hydroxamate
624 sidérophores on Pb(II) adsorption and Fe release from goethite. *Geochim. Cosmochim. Acta* **63**, 3003-
625 3008.
626
627 Lazo D.E., Dyer L.G. and Alorro R.D. (2017) Silicate, phosphate and carbonate mineral dissolution
628 behavior in the presence of organic acids: a review. *Mineral Engineering* **100**, 115-123.

629 Liermann L. J., Kalinowski B. E., Brantley S. L. and Ferry J. G. (2000) Role of bacterial siderophores in
630 dissolution of hornblende. *Geochim. Cosmochim. Acta* **64**, 587-602.

631 Martinez-Luevanos A., Rodriguez-Delgado M., Uribe-Salas A., Carillo-Pedroza F. and Osuna-Alarcon
632 J. (2011) Leaching kinetics of iron from low grade kaolin by oxalic acid solutions. *Applied Clay Science*
633 **51**, 473-477.

634 Mason O., Di Meo-Savoie C., van Nostrand J., Zhou J., Fisk M. and Giovannoni J. (2009) Prokaryotic
635 diversity, distribution and insights into their role in biogeochemical cycling in marine basalts, *ISME J* **2**,
636 231-242.

637 Meyer J. M. and Abdallah M. A. (1978) The fluorescent pigment of *Pseudomonas fluorescens*:
638 biosynthesis, purification and physicochemical properties. *J. Gen. Microbiol.* **107**, 319-328.

639 Morin G.P., Vigier N., Verney-Carron A. (2015) Enhanced dissolution of basaltic glass in brackish
640 waters: Impact on biochemical cycles. *Earth and Planetary Science Letters* **417**, 1-8.

641 Oelkers E. (2001) General kinetic description of multioxide silicate mineral and glass dissolution.
642 *Geochim. Cosmochim. Acta* **65**, 3703-3719.

643 Oelkers E. H. and Gislason S. R. (2001) The mechanism, rates and consequences of basaltic glass
644 dissolution: I. An experimental study of the dissolution rates of basaltic glass as a function of aqueous
645 Al, Si and oxalic acid concentration at 25°C and pH 3 and 11. *Geochim. Cosmochim. Acta* **65**, 3671-
646 3681.

647 Oelkers E. and Schott, J. (1998) Does organic acid adsorption affect alkali feldspar dissolution rates?
648 *Chem. geol.* **151,** 235-245.
649
650 Olsen A. and Rimstidt D. (2008) Oxalate-promoted forsterite dissolution at low pH. *Geochim.*
651 *Cosmochim. Acta* **72,** 1758-1766.
652
653 Orcutt B., Sylvan J., Knab N. and Edwards K. (2011) Microbial ecology of the dark ocean above, at
654 and below the seafloor. *Microbiology and Molecular Biology Review* **75**, 361-422.
655
656 Oulkadi D., Balland-Bolou-Bi C., Billard P., Kitzinger G., Parrello D., Mustin C. and Banon S. (2014)
657 Interactions of three soil bacteria species with phyllosilicate surfaces in hybrid silica gels. *Microbiol.*
658 *Lett.* **354**, 37-46.
659
660 Parrello D., Zegeye A., Mustin C. and Billard P. (2016) Siderophore-mediated iron dissolution from
661 nontronites is controlled by mineral cristallochemistry. *Front. Microbiol.* **7**, Article 423.
662
663 Parruzot B., Jollivet P., Rébiscoul D. and Gin S. (2015) Long-term alteration of basaltic glass :
664 Mechanisms and rates. *Geochim. Cosmochim. Acta* **154**, 28-48.
665 Techer I., Advocat T., Lancelot J. and Liotard J. (2000) Basaltic glass : Alteration mechanisms and
666 analogy with nuclear waste glasses. *J. Nucl. Mater.* **282**, 40-46.

667 Perez A., Rossano S., Trcera N., Verney-Carron A., Huguenot D., van Hullebusch E. D., Catillon G.,
668 Razafitianamaharavo A. and Guyot F., (2015) Impact of iron chelators on short-term dissolution of
669 basaltic glass. *Geochim. Cosmochim. Acta* **162**, 83-98.

670 Perez A., Rossano S., Trcera N., Huguenot D., Fourdrin C., Verney-Carron A., van Hullebusch E. and
671 Guyot F. (2016) Bioalteration of synthetic Fe(III)-, Fe(II)-bearing basaltic glasses and Fe-free glass in
672 the presence of the heterotrophic bacteria strain *Pseudomonas aeruginosa*: impact of siderophores.
673 *Geochimica et Cosmochimica Acta* **188**, 147-162.
674
675 Pokrovsky O., Golubev S. and Jordan G. (2009a) Effect of organic and inorganic ligands on calcite
676 and magnesite dissolution rates at 60°C and 30 atm pCO2. *Chem. Geol.* 265, 33-43.
677
678 Pokrovsky O., Shirokova L., Bénézeth P., Schott J. and Golubev S. (2009b) Effect of organic ligands
679 and heterotrophic bacteria on wollastonite dissolution kinetics. *Am. J. Sci.* 140, 1-7.
680
681 Santelli C., Edgcomb V., Bach W. and Edwards K. (2009) The diversity and abundance of bacteria
682 inhabiting seafloor lavas positively correlates with rock alteration. *Environmental Microbiology* **11**, 86-
683 98.

684 Schalk IJ and Guillon L (2013) Fate of ferrisiderophores after import across bacterial outer
685 membranes: different iron release strategies are observed in the cytoplasm or periplasm depending on
686 the siderophore pathways. *Amino Acids* **44**, 1267-1277.

687 Shirokova L. S., Bénézeth P., Pokrovsky O. S., Gerard E., Menez B. and Alfredsson H. (2012) Effect
688 of the heterotrophic bacterium *Pseudomonas reactans* on olivine dissolution kinetics and implications
689 for CO_2 storage in basalts. *Geochim. Cosmochim. Acta* **80**, 30–35.

690 Schwyn B. and Neilands J. B. (1987) Universal Chemical-Assay for the Detection and Determination
691 of Siderophores. *Anal. Biochem.* **160** 47–56.

692 Spivack A. J. and Staudigel H (1994) Low-temperature alteration of the upper oceanic crust and the
693 alkalinity budget of seawater. *Chem Geol* **115**, 239–247.

694 Staudigel H., Hart S.R. (1983) Alteration of basaltic glass: mechanisms and significance for the
695 oceanic crust seawater budget. *Geochim. Cosmochim. Acta* **47**, 337–350.

696 Stillings L. L., Drever J.I., Brantley S. L and Sun Y. (1995) Rates of feldspars dissolution at pH 3-7 with
697 0-8 mM oxalic acid. *Chem. geol.* **132**, 79-89.

698 Stockmann G. J., Shirokova L. S., Pokrovsky O. S., Bénézeth P., Bovet N., Gislason S. R. and
699 Oelkers E. H. (2012) Does the presence of heterotrophic bacterium *Pseudomonas reactans* affect
700 basaltic glass dissolution rates? *Chem. geol.* **296-297**, 1-18.
701
702 Stroncik N. and Schmincke H. (2001) Evolution of palagonite : Crystallization, chemical changes, and
703 element budget. *Geochem. Geophy. Geosy.* **2**, 365-370.
704
705 Sudek L.A., Templeton A.S., Tebo B.M. and Staudigel H. (2009). Microbial ecology of Fe(hydroxide)
706 mats and basaltic rock from Vailulu'u Seamount, American Samoa. *Geomicrobiol. J.* **26**, 581-596.
707
708 Sudek L.A., Wanger G., Templeton A.S., Staudigel H. and Tebo B.M. (2017) Submarine Basaltic glass
709 colonization by the heterotrophic Fe(II)-oxidizing and siderophore-producing deep-sea bacterium
710 Pseudomonas stutzeri VS-10: The potential role of basalt in enhancing growth. *Front. Microbiol*. **8**,
711 363.

712 Sverdrup H. (2009) Chemical weathering of soil minerals and the role of biological processes. *Fungal*
713 *Biology Reviews* **23**, 94-100.

714 Techer I., Lancelot J., Clauer N., Liotard J. and Advocat T. (2001b) Alteration of a basaltic glass in an
715 argillaceous medium : The Salagou dike of the Lodève Permian Basin (France). Analogy with an
716 underground nuclear waste repository. *Geochim. Cosmochim. Acta* **65**,1071-1086.
717
718 Templeton A. S., Staudigel H. and Tebo B. M. (2005) Diverse Mn(II)-Oxidizing Bacteria Isolated from
719 Submarine Basalts at Loihi Seamount. *Geomicrobiol* **22**, 127–139.

720 Thorseth I., Torsvik T., Torsvik V., Daae F. and Pedersen R. (2001) Diversity of life in ocean floor
721 basalt. *Earth and Planetary Science Letters* **194**, 31-37.
722
723 Torres M.A., West A.J. and Nealson K. (2014) Microbial acceleration of olivine dissolution via
724 siderophore production. *Procedia Earth and Planetary Science* **10**, 118-122.
725
726 Torres M.A., Dong S., Nealson K.H. and West A.J. (2018) The kinetics of siderophore-mediated olivine
727 dissolution. *Geobio*l **00**, 1-16.
728
729 Ullman W. J., Kirchman D. L., Welch S. A. and Vandevivere P. (1996) Laboratory evidence for
730 microbially mediated silicate mineral dissolution in nature. *Chem. Geol.* **132**, 11-17.

731 Uroz S., Calvaruso C., Turpault M.P. and Frey-Klett P. (2009) Mineral weathering by bacteria: ecology,
732 actors and mechanisms. *Trends in Microbiology* **17**, 378-387.

733 Verney-Carron A., Viguier N. and Millot R. (2011) Experimental determination of the role of diffusion
734 on Li isotope fractionation during basaltic glass weathering. *Geochim. Cosmochim. Acta* **75**, 3452-
735 3468.

736 Wang Q., Gao S., Ma X., Mao X., He L. and Sheng X. (2018) Distinct mineral weathering effectiveness
737 and metabolic activity between mineral-weathering bacteria Burkholderia metallica F22 and
738 Burkholderia phytofirmans G34. *Chemical Geology*, in press.

739 Wang X., Li Q., Hu H., Zhang T. and Zhou Y. (2005) Dissolution of kaolinite induced by citric, oxalic
740 and malic acids. *Journal of Colloids and Interface Sciences* **290**, 481-488.

741 Watteau F. and Berthelin J. (1994) Microbial dissolution of iron and aluminium from soil minerals:
742 Efficiency and specificity of hydroxamate sidérophores compared to aliphatic acids. *Soil Biology* **30**, 1-
743 9.

744 Welch S. and Ullman W. (1992) The effect of organic acids on plagioclase dissolution rates and
745 stoichiometry. *Geochim. Cosmochim. Acta* **57**, 2725-2736.

746
747 Wolff-Boenisch D., Gislason S. R., Oelkers E. H., and Putnis C. V. (2004a) The dissolution rates of
748 natural glasses as a function of their composition at pH 4 and 10.6, and temperatures from 25 to
749 74°C.*Geochim. Cosmochim. Acta* **68**(23), 4843-4858.

750 Wolff-Boenisch D., Gislason S.R. and Oelkers E.H. (2004b) The effect of fluoride on the dissolution
751 rates of natural glasses at pH 4 and 25°C. *Geochim. Cosmochim. Acta* **68**, 4571-4582.

752 Wolff-Boenisch D. and Traina S.J. (2007) The effect of desferrioxamine B, enterobactin, oxalic acid,
753 and Na-alginate on the dissolution of uranyl-treated goethite at pH 6 and 25°C. *Chem. Geol.* **243**, 357-
754 368.

755 Wolff-Boenisch D., Wenau S., Gislason S. R. and Oelkers E. H. (2011) Dissolution of basalts and
756 peridotite in seawater, in the presence of ligands, and CO_2: implications for mineral sequestration of
757 carbon dioxide. *Geochim. Cosmochim. Acta* **75**, 5510-5525.

758